SOILS AND FOUNDATIONS Vol. 38, No. 2, 165-177, June 1998
Japanese Geotechnical Society

CENTRIFUGE MODEL TESTS OF NAILED SOIL SLOPES

KOUJI TEI[i], R. NEIL TAYLOR[ii] and GEORGE W. E. MILLIGAN[iii]

ABSTRACT

This paper presents the results of 24 centrifuge model tests of nailed soil slopes and vertical walls, constructed out of dry Leighton buzzard sand. The walls were initially supported by fluid pressure from flexible rubber bags against the face, and excavation was modelled by gradually draining the fluid from the bags. The finished model walls were 200 mm high and were initially tested at 30 g acceleration to correspond to a prototype structure 6.0 m high. If failure was not obtained, the acceleration was increased progressively to a maximum of 80 g. No surcharges were applied.

The main parameters varied in the tests were the wall slope, nail length, nail surface roughness, nail inclination, facing stiffness and facing roughness. Observations were made of the mechanism of failure when it occurred, of soil pressures on the facing, and of pre-failure deformations. Failure was always by pull-out rather than breakage of the nails, and a series of pull-out tests of the model nails was conducted to aid interpretation of the results.

Failure surfaces were seen to have the shape of logarithmic spirals, and limit equilibrium analyses based on these surfaces agreed well with experimental observations. Prior to failure, earth pressures on the facing compared reasonably well with those calculated by Coulomb's method, except at the base of the wall. One test set out to model a full-scale trial wall, and although the construction process could not be exactly modelled in the small-scale centrifuge tests, comparisons were sufficiently good to give confidence in the model test results.

Key words: centrifuge tests, model tests, soil nailing, soil reinforcement (**IGC**: E6/H9)

INTRODUCTION TO MODEL TESTING

Introduction

In earth structures, including nailed slopes, the principal body force which governs deformation and failure is the self weight of the soil. The main advantage of using centrifuge model testing is that an artificially high acceleration field is applied which makes the model material heavier, so that the magnitude and distribution of stress are the same in the model as in the full scale prototype. Thus a centrifuge test can take into account correctly the influence of stress level on the values of friction angle and shear modulus G of the model sand and between the soil and a nail (Garg, 1992). Another important advantage of the centrifuge is that loading on the upper ground surface is not required to cause collapse of a given nailed slope. This is important since the shape and location of the failure surface are strongly dominated by the boundary conditions of the loading.

Shen et al. (1982) may have been the first researchers to use centrifuge techniques to investigate soil nailing. Results of their experiments showed good agreement with their proposed design method, using a limit equilibrium analysis which assumed parabolic failure surfaces in the nailed slope. Stewart (1990) investigated the effect of nails in heavily overconsolidated kaolin using a centrifuge, and found that the mobilization of axial forces in the nails was closely related to the dissipation of negative pore water pressures induced during excavation of the slope. A series of dynamic centrifuge tests was conducted by Tufenkjian et al. (1992). They showed the excellent stability of nailed slopes against seismic loads, and observed a two part wedge failure mechanism in the slopes. Bolton et al. (1978) and Bolton et al. (1982) performed a number of centrifuge tests of a reinforced soil wall, and their main conclusions were:

(1) the peak tension in the zone behind the lower quarter of the facing wall is smaller than that predicted by Rankine's active earth pressure,
(2) even if one reinforcement breaks due to tension, the reinforced soil wall can sustain the earth pressure, as stress re-distribution occurs in the soil,

[i] Senior Geotechnical Engineer, Civil Works Technology Department, Tokyu Construction Co., Ltd., 1-15-21 Shibuya, Shibuya-ku Tokyo 150-0002. (Formerly Research Student, Department of Engineering Science, University of Oxford, UK.)
[ii] Professor of Civil Engineering, Geotechnical Engineering Research Centre, City University, Northampton square, London EC1V 0HB, UK.
[iii] Associate, Geotechnical Consulting Group, 1[A] Queensberry Place, London SW7 2DL, UK. (Formerly University Lecturer, Department of Engineering Science, University of Oxford, UK.)
Manuscript was received for review on October 7, 1996.
Written discussions on this paper should be submitted before January 1, 1999 to the Japanese Geotechnical Society, Sugayama Bldg., 4F, Kanda Awaji-cho, 2-23,,Chiyoda-ku, Tokyo 101-0063, Japan. Upon request the closing date may be extended one month.

(3) as Santamarina (1987) pointed out later, the conventional trapezoidal distribution of vertical earth pressure beneath the reinforced block is shown to be conservative for estimating the lateral earth pressures on the facing wall.

Jaber (1989) performed centrifuge tests and showed that the stability of a reinforced soil wall was affected by the bending stiffness, longitudinal stiffness and continuity of its facing, and suggested simple design methods against the breakage of reinforcement based on the results of the tests, whereby

$$F_s=\frac{nT_{ult}}{\frac{1}{2}K_a\gamma H^2 S_h} \tag{1}$$

where F_s is the safety factor, n is the number of reinforcements in the cross section, T_{ult} is the tensile strength of the reinforcement, K_a is the Rankine earth pressure coefficient, H is the wall height, and S_h is the horizontal spacing of reinforcement. However, because Eq. (1) does not take into account the shape of the failure surface and failure by pull-out of reinforcement, limitations in applying Eq. (1) still remain. Yoo (1988) carried out a number of centrifuge tests on reinforced soil walls, and concluded that the existing design methods for reinforced soil walls appeared to be on the safe side.

Consideration of Similarity Laws for Centrifuge Tests

When the physical scale of a prototype is reduced in a centrifuge model, similarity laws relating the prototype and the model should be established and satisfied as far as is practicable. Gassler (1987) suggested the following similarity law, based on considerations of bending

$$\frac{(E_aI)_m}{(E_aI)_p}=\frac{\gamma_m}{\gamma_p}\left(\frac{1}{N}\right)^5 \tag{2}$$

where E_aI and γ are the bending stiffness of the reinforcement and the unit weight of the soil, the suffices p and m denote the prototype and centrifuge model respectively and N is the scaling factor.

Tei (1993) derived an alternative similarity law by considering the stress and strain in a nail and the friction along it:

$$\frac{(R_aE_a)_p}{(R_aE_a)_m}=N \tag{3}$$

where R_a is the radius of the nail. Taniguchi et al. (1987) and Ovesen (1984) derived the same similarity law as Eq. (3) from different assumptions. On the basis of a simple anchor theory (Bolton et al., 1982), the following similarity laws for breakage at the connection between a nail and the facing wall, and for the pull-out of nails, are obtained:

$$\frac{(T_{ult})_p}{(T_{ult})_m}=N^2\left(\frac{D_m}{D_p}\right)^2,\quad \frac{(f^*)_p}{(f^*)_m}=N^2\frac{D_ml_m}{D_pl_p} \tag{4}$$

where T_{ult} is the tensile strength of a nail contained in a body of soil with dimensions S_v and S_h, D and l are the diameter and length of the nail respectively, and $f^*=\tau_{max}/\sigma_m$ is the apparent friction coefficient for the nail. Here τ_{max} and σ_m are the maximum shear stress and mean normal stress on the nail respectively.

EXPERIMENTAL PROCEDURE

Prototype wall

The general arrangements of the model walls for the centrifuge tests were designed to correspond to a full scale test performed by Gassler and Gudehus (1983), as shown in Fig. 1. The prototype wall was 6.0 m high, with a face angle of 80° to the horizontal, and contained five rows of primary reinforcement. It was constructed in uniform sand with the properties given in Table 1. Nails, at an inclination $\Gamma=10°$ to the horizontal, were 22 mm diameter deformed steel bars grouted into boreholes of diameter 55 mm, at vertical and horizontal spacings of 1.1 and 1.2 m respectively. The wall facing consisted of shotcrete 100 mm thick, with nail loads transmitted through 200 mm square steel plates. Instrumentation included several earth pressure cells on the facing, inclinometers, and strain gauges on the nails.

Model walls

The model walls were constructed with dry yellow Leighton Buzzard 50/100 sand. This is a uniform quartz laboratory sand passing the No. 50 sieve (0.21 mm) but retained on the No. 100 sieve (0.15 mm). It is more important to obtain similar mechanical behaviour of the model and prototype sands than to scale the particle sizes exactly. A geometric scaling factor $N=30$ was chosen for the centrifuge tests so that the diameter D of the model

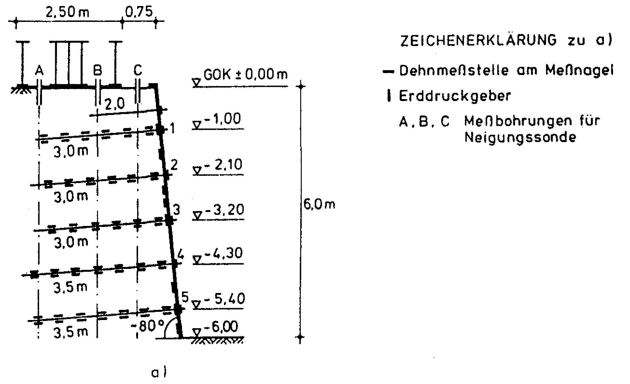

Fig. 1. Prototype test carried out in Germany (after Gassler, 1987)

Table 1. Properties of sand used in the prototype test (after Gassler, 1987)

γ_i (kN/m³)	γ_d (kN/m³)	e	D_r (%)	D_{50} (mm)	ϕ'_p (deg.)	ϕ'_{cv} (deg.)
15.6	14.8	0.83	62	0.3	40.5	35

Note: ϕ'_{cv}=critical state friction angle obtained by triaxial compression tests.

nails was not too small in comparison with the size of the sand grains. The relative density D_r of the Leighton Buzzard sand in the centrifuge tests was measured to be about 88–93%, which is almost the same as that of the sand (D_r=92–94%) used in pull-out tests on the model nails, described by Tei (1993). The width and height of the walls were 192 mm and 200 mm respectively.

Two types of nail, of circular cross section, were used for the centrifuge tests:—

(1) A rough-surface nail made from a stainless steel bar with a diameter D=1 mm to which was glued a layer of sand bringing the total diameter D_n to 1.7 mm.
(2) A smooth-surface nail made of stainless steel bar with a diameter D=3 mm; this diameter is almost twice that of the rough nail, to avoid extremely low pull-out forces.

With the scaling factor N=30, the nails with D=1 mm and D_h=1.7 mm nearly satisfy the similarity law in Eq. (3) for the stress/strain of a nail. All nails in the centrifuge tests were equipped with a circular head plate made of steel with a diameter of 12 mm and thickness of 0.5 mm.

In order to investigate the influence of the thickness and roughness of the wall facing on the stability of nailed slopes, four types of facing were used to cover the whole area of the slope surface. Flexible facings were made of perspex with a thickness of t=0.6 mm, and stiff facings of perspex with a thickness of t=5.2 mm; each of these could be either smooth-faced or rough-faced, the latter being obtained by gluing sand to the surface. From interface tests, it was found that for a smooth-faced wall the interface friction angle δ_w was 15°, while for a rough-surface wall δ_w was 30°. At 30 g acceleration, the relative stiffness of the flexible facing in the model (t=0.6 mm) and the shotcrete facing of the prototype were almost the same.

Centrifuge Test Procedure

The internal dimensions of the strong box used in the centrifuge tests were 375 × 550 × 200 mm. The first stage of sample preparation involved pluviating the sand in a standard fashion, using a hopper with perforated plates. After a sand layer of 70 mm thickness had been poured in the lower part of the strong box, the wall facing with 25 nails was placed in the required position on the sand layer (Fig. 2). The nails were inserted through 25 holes of 5 mm diameter in the facing. Pluviation of the sand behind the facing was then completed. During this stage, the wall facing was temporarily supported by shaped wooden blocks. On completion of pluviation, support of the facing was transferred to two rubber bags filled with water, one each side of the instrument array in plan.

During tests, measurements were made of the earth pressures on the facing, using five miniature earth pressure cells, and of the horizontal displacements of the facing and vertical displacements of the upper ground surface, using nine displacement transducers (LVDT type), as shown in Fig. 3. The diameter and thickness of the miniature earth pressure cells were 5 mm and 0.2 mm respectively, and the cells were fixed on the back of the wall facing. Extension rods passing between the two rubber bags transferred horizontal movement from the central part of the wall to the horizontal transducers mounted in the gantry. Photographic measurements of the displace-

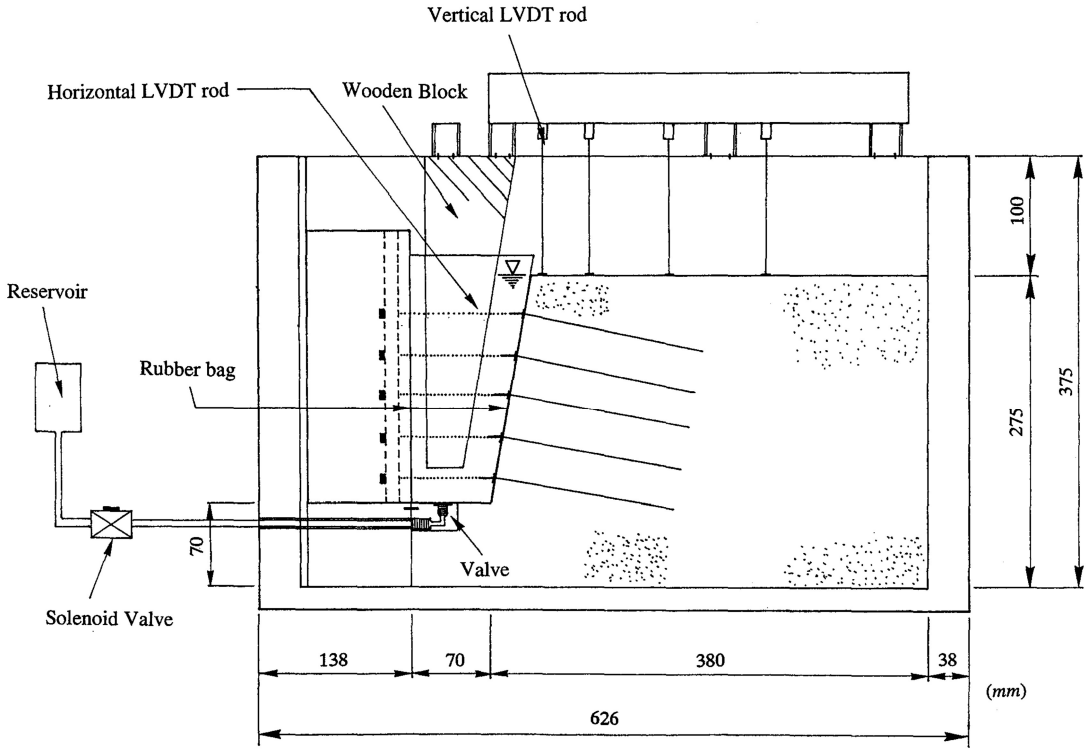

Fig. 2. General arrangement of centrifuge test box

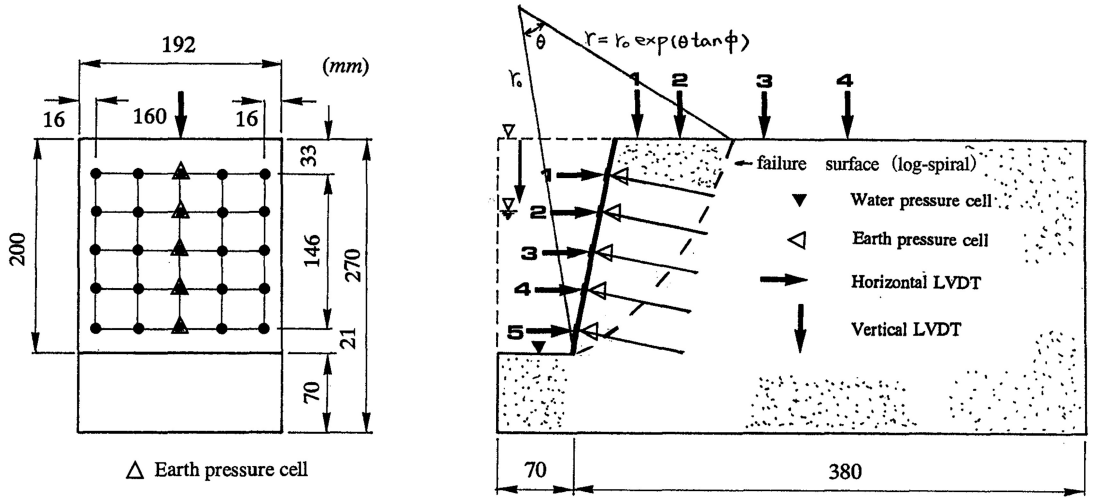

Fig. 3. Arrangement of nails and instruments in centrifuge tests

Table 2. Details of centrifuge tests

Test	β (°)	Nail l (cm)	Nail type	Nail Γ (°)	Facing stiffness	Facing roughness	N_f (g)
A6.5-F-R	80	6.5	Rough	0	Flexible	ROUGH	30
A6.5-R-R	80	6.5	Rough	0	Rigid	ROUGH	36
A'6.5-R-R	80	6.5	Rough	10	Rigid	ROUGH	45
A7.0-R-S	80	7.0	Rough	0	Rigid	SMOOTH	NO
A18-F-R	80	18.0	Smooth	0	Flexible	ROUGH	33
A18-R-R	80	18.0	Smooth	0	Rigid	ROUGH	30
A20-F-S	80	20.0	Smooth	0	Flexible	SMOOTH	72
A'20-F-S	80	20.0	Smooth	10	Flexible	SMOOTH	56
A20-R-S	80	20.0	Smooth	0	Rigid	SMOOTH	NO
A'20-R-S	80	20.0	Smooth	10	Rigid	SMOOTH	64
A'20-R-R	80	20.0	Smooth	0	Rigid	ROUGH	NO
A20-F-R	80	20.0	Smooth	0	Flexible	ROUGH	NO
A*18-F-R	80	18.0	Smooth	0	Rigid	ROUGH	24
Proto-F	80	10.0/11.6	Rough	0	Flexible	ROUGH	NO
Proto-R	80	10.0/11.6	Rough	0	Rigid	ROUGH	NO
V7.0-F-R	90	7.0	Rough	0	Flexible	ROUGH	30
V'7.0-F-R	90	7.0	Rough	10	Flexible	ROUGH	30
V7.0-R-R	90	7.0	Rough	0	Rigid	ROUGH	30
V8.0-F-S	90	8.0	Rough	0	Flexible	SMOOTH	NO
V8.0-R-S	90	8.0	Rough	0	Rigid	SMOOTH	NO
V8.0-F-R	90	8.0	Rough	0	Flexible	ROUGH	73
V8.0-R-R	90	8.0	Rough	0	Rigid	ROUGH	NO
V8.5-R-S	90	8.5	Rough	0	Rigid	SMOOTH	NO
V20-F-S	90	20.0	Smooth	0	Flexible	SMOOTH	1
V23-F-S	90	23.0	Smooth	0	Flexible	SMOOTH	30

ments of markers placed in the sand were taken through the perspex side wall of the strong box.

During the test, the centrifuge acceleration was first gradually increased from 1 g to 30 g over a period of about two minutes. Wall construction was then modelled by draining the water from the two rubber bags through 8 mm diameter holes in their base to a reservoir, by electrically opening a solenoid valve during flight. This took about 20 seconds, while the acceleration was kept constant at 30 g. If collapse of the slope was not observed after all the water had been drained from the rubber bags, the acceleration was again increased gradually until failure occurred or a maximum value of 80 g was reached.

RESULTS OF CENTRIFUGE TESTS

Failure Conditions

A total of 24 tests on nailed slopes was performed using the centrifuge. Details of the tests are summarised in Table 2, together with the accelerations N_f at which overall failure or excessively large displacements of the nailed slope were observed. In Table 2, β, l, and Γ are the angle of the wall to the horizontal, the length of the nails, and the angle of the nails to the horizontal respectively. All failing slopes collapsed due to the inadequacy of the total anchorage length of the nails beyond the failure surface, rather than by tensile failure of the reinforcement. Observed failure surfaces were well described by logarithmic spirals passing through the toe of the wall, as shown in Fig. 3. It was commonly observed during the tests as the centrifuge acceleration increased that several minor failure surfaces developed progresively, followed by the collapse of the entire nailed slope. Although well-defined shear bands, of thickness $h=10$–20 mm, developed along the failure surfaces, it is interesting to note that the post-test deformation of the nails which extended beyond the failure surfaces showed no distinguishable bending deformation. This result suggests that sharp bending of a nail with significant plastic deformation, and consequently large local shear forces in the nail, can be expected only after excessive displacements have been allowed in the nailed slope. However when using nails with small bending stiffness, plastic deformation of nails along the failure surface could be significant.

Influence of Simulated Excavation

Results of the centrifuge tests are presented in Figs. 4(a)–(c), which show the relations between draining of the water (simulating excavation), the elapsed time T from the beginning of the tests, and (a) the horizontal displacement of the facing, (b) the vertical displacement of the upper ground surface, and (c) the horizontal earth pressures on the facing wall, respectively. The horizontal displacements δ_h of the facing during the increase in acceleration from 1 g to 30 g were found to be nearly zero, due to the external support provided by the rubber bags filled with water. Both the horizontal displacements of the facing and the vertical displacements of the upper

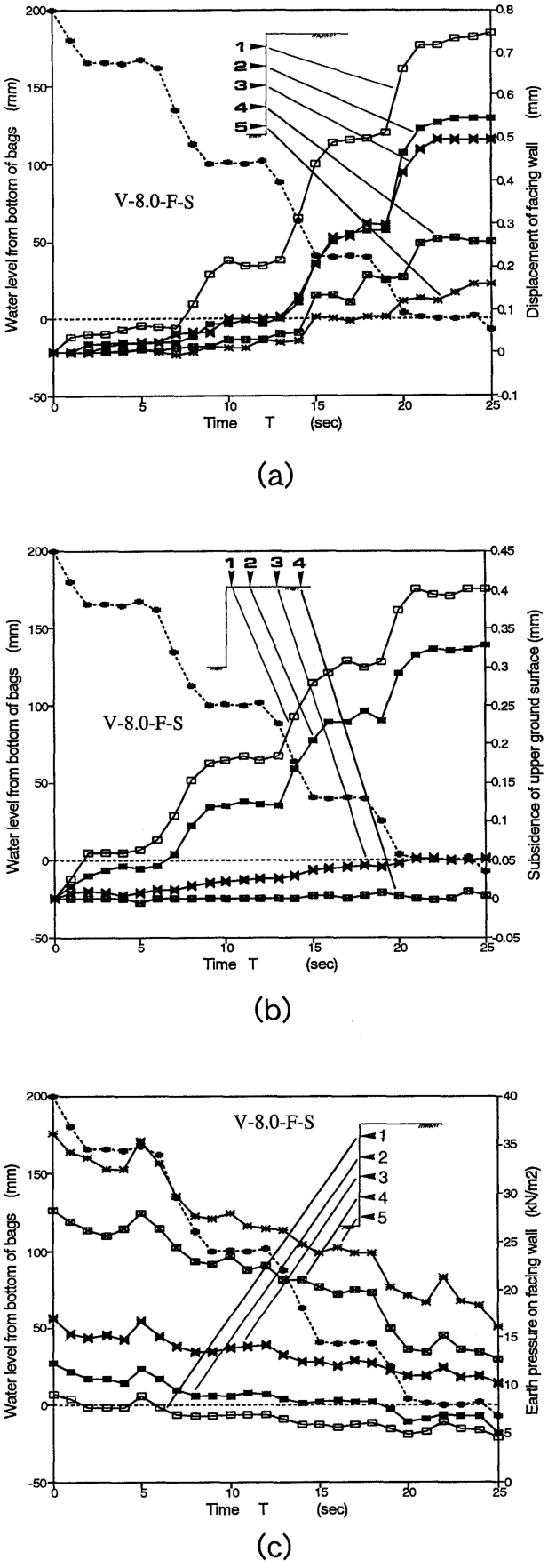

Fig. 4. Typical progress of test during simulated excavation: (a) horizontal displacements of facing, (b) surface settlements, (c) earth pressures

ground surface are closely linked to the process of excavation, and therefore to the earth pressure P_h on the facing. The reductions in earth pressure during excavation varied with depth below the ground surface. A decrease in initial earth pressure of more than 55% was observed in the lower part of the wall, while the decrease was about 35–50% in the upper part of the wall. The average earth pressure after excavation was about 50% of the initial value.

Horizontal Displacements of the Facing

Typical horizontal displacements of the wall are shown in Fig. 5, for the four types of facing: stiff-smooth, stiff-rough, flexible-smooth and flexible-rough. One example is given to show the increase in displacement as the effective gravity is increased above 30 g. For all of the centrifuge tests shown, the largest horizontal displacements were observed at the top of the wall, irrespective of the stiffness and roughness of the facing, and length and roughness of the nails. This observation is commonly reported in practice, for example by Jones (1990). The deflected shapes of the walls with flexible facings were found to be very similar to those of flexible cantilever sheet-pile walls in which the bending stiffness of the wall is very significant (Bransby and Milligan 1975). The magnitudes of the horizontal displacements observed in the nailed slopes were, however, much less than those of flexible cantilever walls at 1 g for which horizontal displacements of 4 mm to 15 mm at the top of the wall were observed for a wall height of $H=300$ mm with 14/25 dense Leighton Buzzard Sand, (Milligan 1974). The most flexible wall used by Milligan was 3 times stiffer than the flexible facing in the current centrifuge tests. However, the flexible cantilever walls produced more than 10 times the horizontal displacements of the nailed slopes in the centrifuge tests. It is, therefore, reasonable to suggest that in a stable nailed slope the nails can decrease the magnitude of the horizontal displacement of the facing in comparison with an unreinforced slope.

Another important feature of Fig. 5 is that some horizontal displacement occurred at the bottom of the walls, and these horizontal displacements were not negligible, especially for the flexible facing. This result indicates that a nailed slope cannot be seen as a cantilever wall nor a ground anchored wall, in which there is usually a point of fixity in the wall embedded in the sand. For the flexible walls, the horizontal displacements combine rotation, sliding, and bulging due to the bending of the facing.

It is of interest to observe how the type of facing and length of nails can affect the magnitude of the horizontal displacements. Maximum horizontal displacements of the wall for the four types of facing, after excavation at an acceleration of 30 g, are shown in Fig. 6, and for different lengths of nail in Fig. 7. The following trends are shown in both figures:—

(1) Horizontal displacements are essentially independent of nail length except that the smallest displacements were obtained with long nails and a stiff facing. Since the maximum stress level of the soil in the centrifuge tests is small compared to the tensile strength and axial stiffness of the nail, most of the

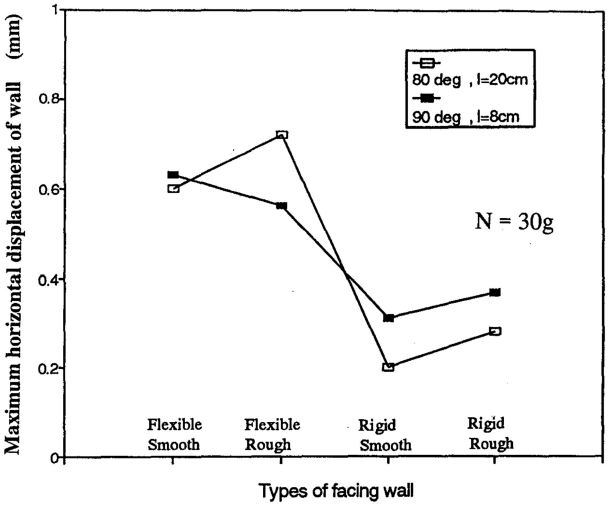

Fig. 6. Horizontal displacements related to facing roughness and flexibility

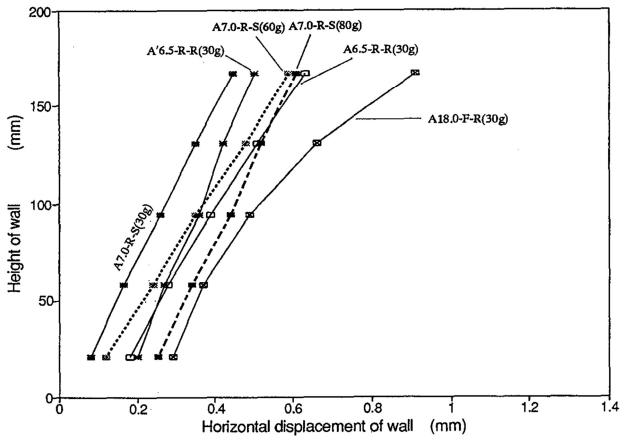

Fig. 5. Profiles of horizontal wall displacements

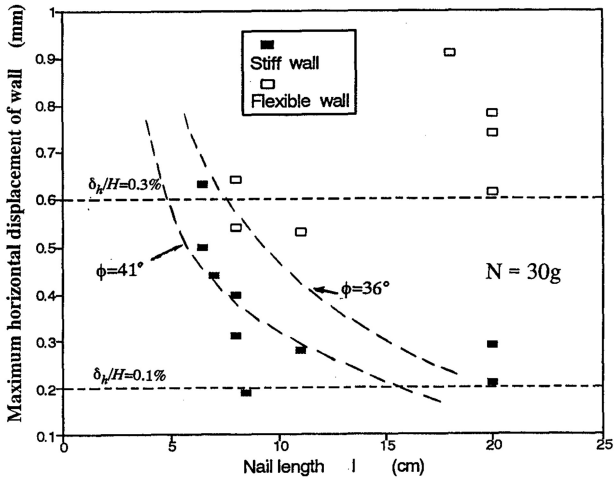

Fig. 7. Horizontal displacements related to nail length

horizontal displacements of the walls were not caused by the elongation of the nails, but by pull-out of the nails due to the earth pressure.

(2) Roughness of the facing does not seem to affect the magnitude of the displacement of the wall, although there is a clear distinction between the stiff and flexible facings.

(3) For nailed slopes with a stiff facing, unlike those with a flexible facing, the displacement ratios δ_h/H are mostly in a range of 0.1–0.3%, as commonly reported in practice.

(4) Therefore, in order to minimize the horizonal displacements of the wall, it is recommended that the length of the nails, the friction between the soil and the nails, and the bending stiffness of the facing be increased.

From simple anchor theory (Bolton et al., 1982) applied to a smooth-faced vertical wall, equilibrium of the axial forces on an individual nail is given by:—

$$K_a\sigma_v S_v S_h=\pi Dl\tau=\pi Dl\frac{\delta_h}{a(\sigma_v)+b(\sigma_v)\delta_h} \qquad (5)$$

where $S_v=3.65$ cm and $S_h=4.00$ cm are the vertical and horizontal spacings of the nail in the tests, $D=1.7$ mm is the diameter of the nail, K_a is Rankine's active earth pressure coefficient, and τ and σ_v ($=22.7$ kN/m^2) are the shear and vertical stresses on the nail, respectively. The last part of this equation comes from fitting hyperbolic curves to the results of pull-out tests. Values of $a=0.022$ cm^3/N and $b=0.120$ cm^2/N were obtained from pull-out test data for a corresponding vertical stress (Tei, 1993), and two possible values of friction angle ϕ (36° and 43°) assumed. The horizontal displacements calculated using this equation are also plotted in Fig. 7. It is clear that both the length l of the nails and the friction angle ϕ strongly influence the calculated displacement of the wall. Although the influence of the stiffness of the facing was not considered, it appears that reasonable estimates of the displacements in the centrifuge tests can be made using Eq. (5), for walls with stiff facings. Displacements of flexible walls are somewhat different because the earth pressure distributions are somewhat different and the deflection of the facing is not negligible.

Vertical Displacement of the Upper Ground Surface

Figure 8 shows the increments of vertical displacement of the upper ground surface due to excavation at 30 g. The limiting stress and velocity characteristics (Bransby and Milligan, 1975) for the ideally smooth facing are also shown for the vertical wall. Assuming that the direction of the principal strain increment is vertical, velocity characteristics are inclined at $(45°-\psi/2)$ either side of vertical. The vertical displacements observed were always largest at the LVDT closest to the facing, located 20 mm from it, and gradually decreased further away from the facing. There was little or no vertical displacement observed at the LVDT furthest from the wall, which is located outside the zone of the velocity characteristics.

The deformations of the soil behind a wall have been

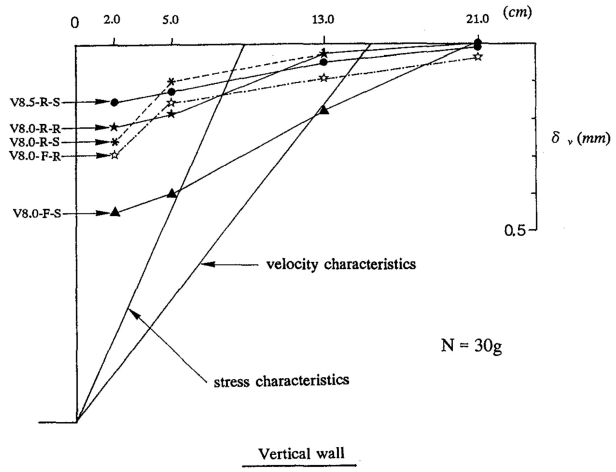

Fig. 8. Surface settlement profiles

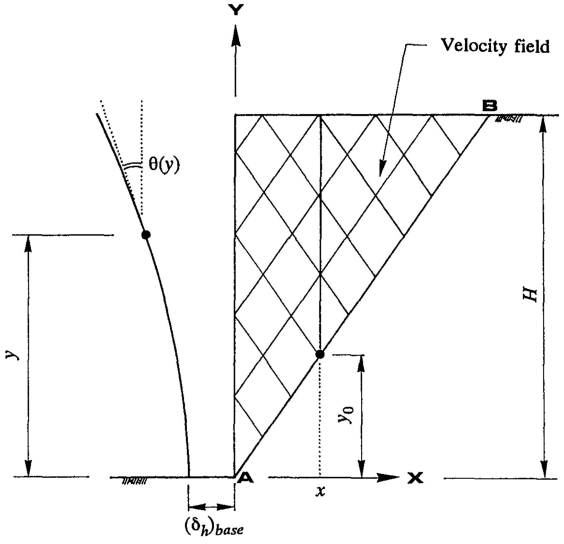

Fig. 9. Calculations of surface settlements from facing displacements

found to be related to the deflection of the facing (Milligan and Bransby, 1975). It can be shown that the vertical displacement δ_v at any point within the region of the velocity field, is given by

$$\dot{\delta}_v=\tan(\pi/4-\psi/2)\left\{\int_{y_0}^{H}\theta(y)\,dy+(\dot{\delta}_h)_{\text{base}}\right\} \qquad (6)$$

where the various terms are as defined in Fig. 9. The increments of vertical displacement measured in the centrifuge tests and those calculated from the observed movements of the facing, at the point of the vertical LVDT No. 1, are shown in Fig. 10, which includes results for both the vertical and inclined walls. The agreement between the measured and calculated vertical displacements is better for the smaller vertical displacements, in the range of 0–0.5 mm. Larger discrepancies between the results were found for a range of $\delta_v>0.5$ mm. It is surprising that reasonably good predictions, especially for the small vertical displacements, were made for the inclined walls as

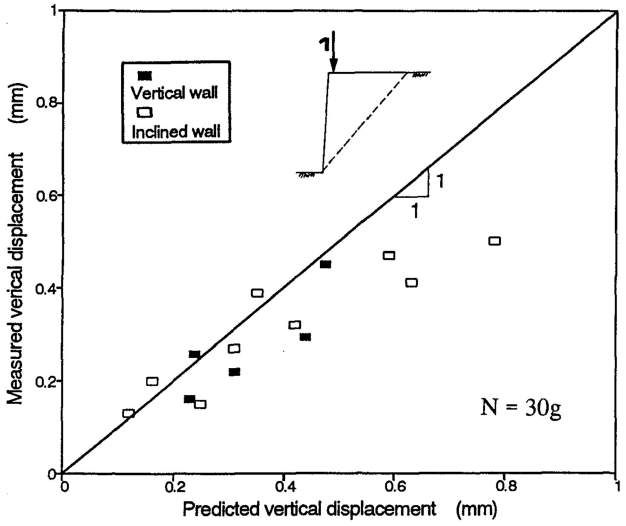

Fig. 10. Calculated and measured surface settlements

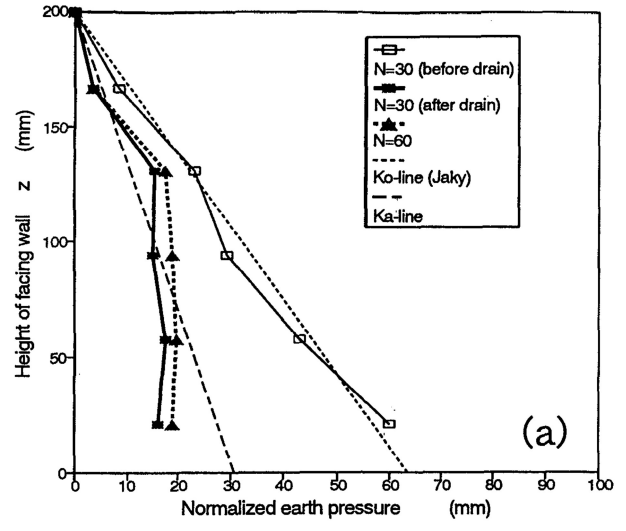

V8.0-R-R

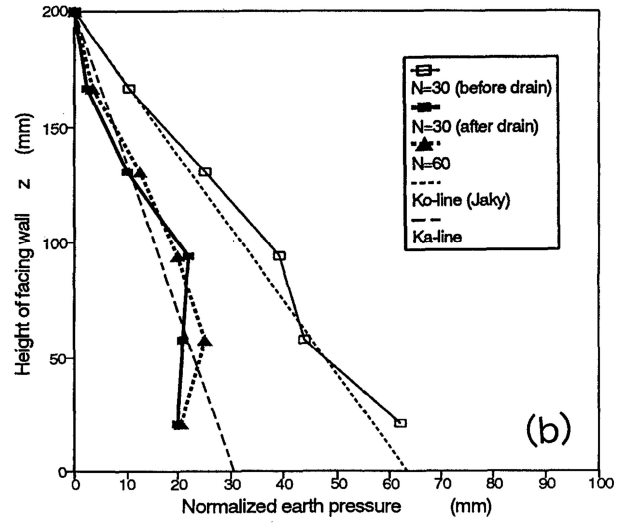

V8.0-F-R

Fig. 11. Distributions of earth pressure: (a) Rigid facing, (b) Flexible facing

well as for the vertical walls using this simple analysis with hand calculations. These results are also consistent with the findings of Bransby and Milligan (1975) that good predictions could be made even for the cantilever sheet pile walls with a rough surface, for which the velocity characteristics should be curved near the facing.

Earth Pressures on the Facing

Figure 11 shows typical examples of distributions of the normalized earth pressure ($p/N\gamma$) at $N=30$ for the four types of facing reinforced with rough nails of length $l=8.0$ cm, where

$$\frac{p}{N\gamma}=K_a z. \tag{7}$$

In Eq. (7), p is the measured horizontal earth pressure on the facing, γ is the unit weight of the soil, K_a is the earth pressure coefficient determined from Rankine's theory, and z is the vertical distance from the upper ground surface. In the centrifuge tests, before draining the water at 30 g acceleration, slightly larger magnitudes of the earth pressures were observed on the facing than the at-rest values p_0, estimated by Jaky's formula (1944) and assuming a plane strain friction angle $\phi_{ps}=43°$. This may be due to the fact that the rubber bags, filled with water, tended to push the facing into the slope. On the other hand, after draining the water, very large decreases in the earth pressures were observed. The centroid of the horizontal earth pressure distribution is located at about $0.55H$–$0.6H$ from the top of the wall, which is a little higher than $2/3H$ for a hydrostatic distribution but slightly lower than $0.5H$–$0.55H$ suggested by Terzaghi and Peck (1948) for a strutted wall in sand. The active earth pressures calculated by Coulomb's theory, assuming a hydrostatic earth pressure distribution, a friction angle for the soil of $\phi=43°$ and an angle of wall friction $\delta_w=30°$ for the rough facing walls, are also shown in Fig. 11. The Coulomb earth pressure is always conservative for the lower part of the wall, where the calculated earth pressures are 20–50% larger than those measured, but this is not usually the case for the upper and middle parts of the wall. No distinct influence of the stiffness of the facing was observed with regard to the horizontal earth pressures.

Ho and Rowe (1992) pointed out that when the horizontal shear force transmitted to the soil below the base of the reinforced soil is included, total earth pressures on a reinforced soil wall will become nearly equal to those calculated by Coulomb's theory. While this approach was found to provide generally conservative total earth pressures for the nailed slopes, individual nails in the upper and middle parts of the wall may suffer larger earth pressures than those calculated using Coulomb's theory. At the same time, the lowest nail does not necessarily provide the lowest factor of safety for pull-out and breakage of an individual nail. This indicates that:

(1) assuming hydrostatic distribution for the horizonal earth pressures produces a conservative estimate for the overall quantity of the nails for the lower part of

the facing wall, and

(2) all the possible failure surfaces passing through the middle and upper parts of the wall should be examined to check whether the quantity of nails can provide sufficient nail forces against the horizontal earth pressures on the facing.

Comparison of Results between the Centrifuge and Prototype Tests

Details of the prototype tests performed by Gassler (1987), have been given above. The horizontal displacements of the wall in the prototype test and centrifuge tests after completion of excavation at the acceleration of 30 g are shown in Fig. 12. In the centrifuge tests, only the rough facing walls are considered because the shotcrete wall in the prototype test was assumed to be rough. For these comparisons, the displacements of the prototype test are scaled down by the factor $N=30$. The agreement between the results of the prototype and centrifuge tests is generally good. The displacement ratio for the prototype tests was $\delta_h/H=0.23\%$, which is in good agreement with in-situ measurements.

It appears that in comparing the shape of the horizontal wall displacements, the shotcrete wall in the prototype tests is more closely modelled by the rigid facing than by the flexible facing, although the magnitude of δ_h is closer to that for the flexible wall in the centrifuge tests. In the prototype tests, the shotcrete wall exhibited bending deformation as well as nearly 3 mm of horizontal displacement at the bottom and 1.8×10^{-3} rad of rotation about its toe. The greater horizontal displacement observed in the prototype test may be partly due to the different construction sequences between the prototype and centrifuge tests. In the former, the nails and shotcrete facing were constructed in stages after excavation of the slope, while all of the nails and the facing had already been placed in the slopes in the centrifuge tests.

Figure 13 compares the distribution of normalized

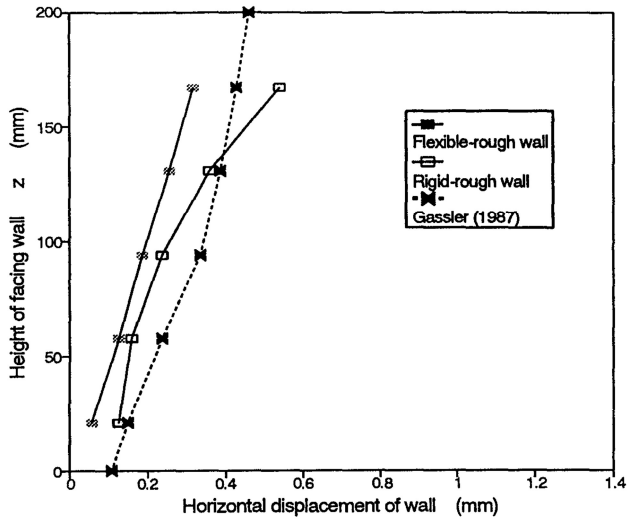

Fig. 12. Horizontal displacements of prototype wall and centrifuge models

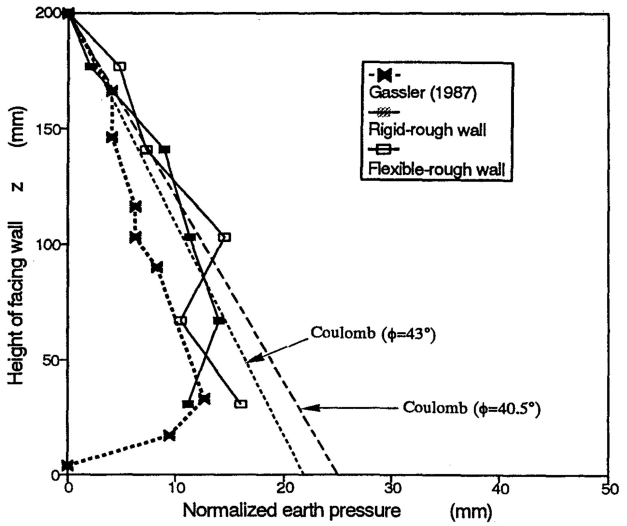

Fig. 13. Earth pressure distributions, prototype wall and centrifuge models

earth pressure ($p/N\gamma$) in the centrifuge and prototype tests, together with the Coulomb earth pressure distributions. Although the total magnitude of the normalized earth pressures differed between the prototype and centrifuge tests, the distributions of horizontal earth pressure were similar for both in that earth pressures were observed to be less than those calculated by Coulomb theory, assuming a hydrostatic distribution with wall height. The deviations of the measured total earth pressures from Coulomb's theory are not negligible, especially for the prototype test, in which only about 50% of the Coulomb earth pressure was observed. Possible reasons for this are:—

(i) some stress relief of the nailed slope due to excavation had already occurred in the prototype test before the earth pressure cells were placed behind the shotcrete wall;

(ii) the earth pressures were reduced by slight cohesion in the soil;

(iii) there was a transfer of stress into the foundation from the soil behind the wall. In fact, a reading of zero was obtained from the lowest earth pressure in the slope. Similar observations have often been made from in-situ measurements, such as reported by Plumelle et al. (1989).

STABILITY ANALYSES OF THE CENTRIFUGE TESTS

Failure Mechanisms

The data on the failure accelerations of the nailed slopes are now compared with the results of a conventional limit equilibrium analysis based on the observed failure mechanisms in the tests, with the objective of investigating the appropriate design procedure for soil nailing. The development of several failure surfaces progressively from the facing to the interior of the nailed slope during the centrifuge tests suggests that it is necessary to

find the most critical failure surface, with the smallest factor of safety (F_s) min, among many possible failure surfaces, instead of simply determining a unique failure surface which produces the maximum total earth pressure on the facing. The shapes of observed failure surfaces in the centrifuge tests were precisely represented by logarithmic spirals from the toe of the nailed slope to the upper ground surface. The logarithmic spiral was also found to be a suitable failure mechanism for reinforced soil walls by Leschinsky (1992).

Prediction of Failure Accelerations from the Limit Equilibrium Analyses

The apparent friction coefficient f^* of the nails under an applied vertical stress σ_v was determined, from pull-out tests of a nail and direct shear tests of the sand, as:—

for $0\ \text{kN/m}^2 \le \sigma_v \le 75\ \text{kN/m}^2$,

Rough nails: $f^* = 2.80 - 2.80 \times 10^{-3}.\ \sigma_v$,

Smooth nails: $f^* = 0.26 - 2.60 \times 10^{-4}.\ \sigma_v$

for $75\ \text{kN/m}^2 \le \sigma_v \le 250\ \text{kN/m}^2$,

Rough nails: $f^* = 2.59 - 1.77 \times 10^{-3}.\ (\sigma_v - 75)$,

Smooth nails: $f^* = 0.24 - 2.57 \times 10^{-4}.\ (\sigma_v - 75)$

where, in the centrifuge tests, the vertical stress σ_v on the nail is calculated as

$$\sigma_v = N\gamma Z. \tag{9}$$

A range of 36° to 41° for the friction angle of the soil was determined for the limit equilibrium analyses of the centrifuge tests, for the following reasons (Tatsuoka 1987):—

(i) the average vertical stress at the mid-height of the slope is 50 to 140 kPa, giving $36° \le \phi_{ds} \le 38°$.

(ii) the angle of friction is affected by anisotropy, giving $41° \le \phi_{ds} \le 44°$.

(iii) progressive failure tends to reduce the angle of friction towards the critical state value, $\phi_{cv} = 33°$–$36°$ (Bolton, 1986).

These values represent lower and upper bounds on the available soil strength. The stability of the slopes was estimated from the following factor of safety F_s:

$$F_s = \frac{\textit{total available nail force}}{\textit{total required nail force}} = \frac{T_{ava}}{T_{req}}. \tag{10}$$

The contribution of the shear resistance of the nail is ignored in the total required force T_{ava} because bending of the nails in the centrifuge tests was not observed. The total available force T_{ava} is determined from the total pull-out force of the nails beyond the failure surface as

$$T_{ava} = \sum_i T_i l_i = \sum_i \pi D_i l_i (\sigma_m)_i f_i^* \tag{11}$$

in which T_i is the maximum pull-out resistance per unit length of a nail, l_i is the length of a nail beyond the failure surface, D is the diameter of a nail. The mean stress σ_m is approximately estimated using Jaky's formula (1944), as

$$\sigma_m = \frac{(1+K_0)\sigma_v}{2} = 0.659\sigma_v. \tag{12}$$

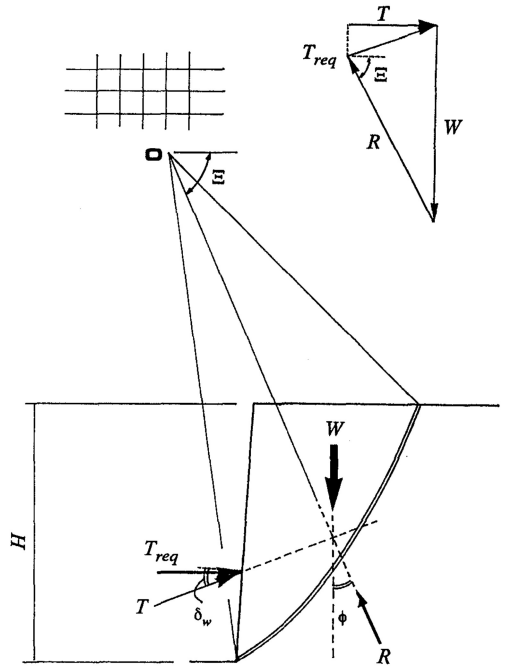

Fig. 14. Theoretical stability analysis

The total required force T_{req} which is necessary to stabilize the slope is calculated using the force polygon for the observed failure surface (Fig. 14). The derivation of the equation of the logarithmic spiral from the observed failure surface in the centrifuge tests was carried out by trial-and-error.

To summarize, the following assumptions were made in the analyses:—

(1) Friction angles of the soil were 36° and 41°, for the lower and upper bounds, respectively.

(2) Location of the centroid of total required force T_{req} was at two thirds of the height H of the wall from the upper ground surface.

(3) Angles of roughness for the wall facings were $\delta_w = 15°$ and 30° for the smooth and rough facings respectively.

(4) Apparent friction coefficients f^* for the smooth and rough nails for the corresponding vertical stresses were derived from pull-out test data.

(5) Orientation of the nails was horizontal.

Figure 15 shows a typical relationship between the centrifuge acceleration N from 30 g to 80 g, the total required force T_{req} per width of the horizontal nail spacing ($b = 40$ mm) for friction angles of 36° and 41°, and the total available force T_{ava}. These calculations of the required forces T_{req} and available forces T_{ava} were based on the failure surfaces observed in the centrifuge tests. On the other hand, iterative calculations were required to obtain the minimum factor of safety (F_s) min and the corresponding forces T_{req} and T_{ava} for those tests in which failure did not occur even after achieving 80 g acceleration. Figure 15 also shows plots of the factors of safety obtained from Eq. (10) using the two friction angles, $(F_s)_{36}$, $(F_s)_{41}$; their average ($(F_s)_{ave}$); and a point of ob-

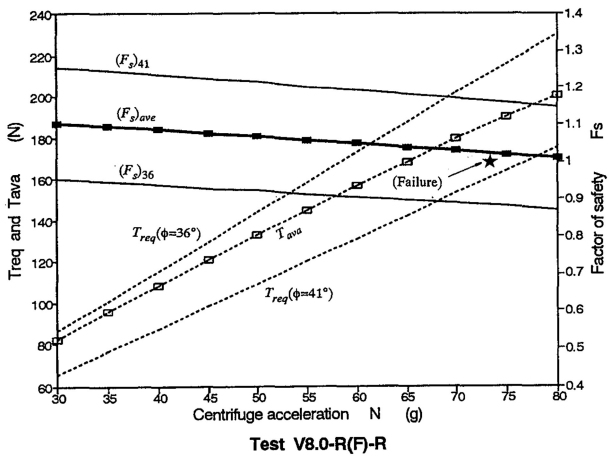

Fig. 15. Required and available reinforcement forces and factors of safety

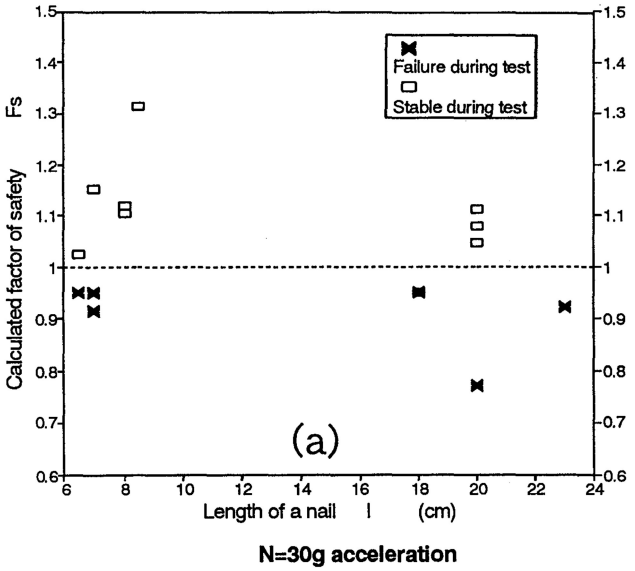

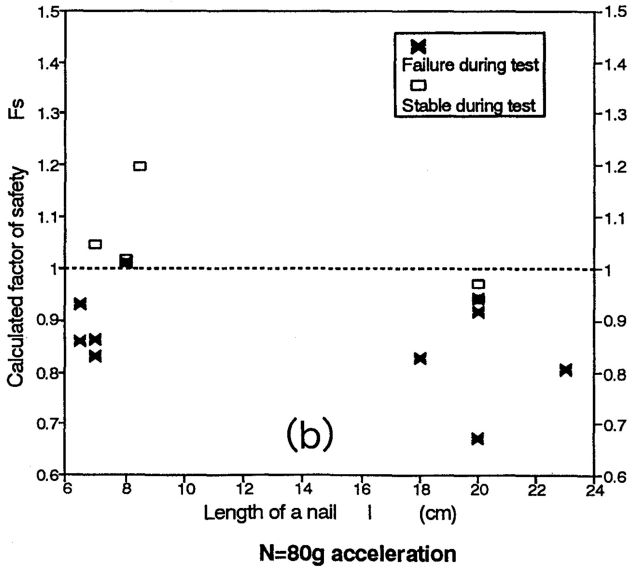

Fig. 16. Observed slope failures and calculated factors of safety: (a) at 30 g, (b) at 80 g

served failure acceleration. For all the centrifuge tests, the actual failure accelerations were found to fall within the range for which the calculated factors of safety lay between $(F_s)_{36}=1.00$ and $(F_s)_{41}=1.00$. However it should be noted that a difference of only 5° in the friction angle produces a difference in the factor of safety of 20 to 30%.

Figure 16 compares the average factors of safety $(F_s)_{ave}$ with the existence of a failure of the slope for each test, for centrifuge accelerations of 30 g and 80 g. In the figure, the cross symbols indicate the failure of nailed slopes at less than the given acceleration N g, while the empty squares indicate stable nailed slopes at the given acceleration. Similar plots may be constructed for intermediate values of N. Generally the agreement between the theory based on the limit equilibrium analysis and the results of the centrifuge tests is excellent, though the theoretical calculations tend to be a little conservative for the slopes with long nails. This close agreement indicates that limit equilibrium analysis can be used accurately to evaluate the factor of safety F_s of a nailed slope when a suitable failure mechanism, reasonable friction angle of the soil and the correct peak pull-out forces for the nails are used in the analysis. Further, the limit equilibrium analysis can successfully take into account the influence of the roughness of the facing, in the same way as in the analysis of conventional retaining walls.

Failure of the Prototype Wall

In the prototype test carried out in Germany, a uniform surcharge q was applied at the top of the nailed slope, and achieved a value of $q=100$ kN/m^2 when the wall collapsed. From the observed failure surface, as shown in Fig. 17, the appropriate equation of a logarithmic spiral was calculated as

$$r=4.97 \exp[(\theta-0.881)\tan\phi] \quad (\textit{units}: \text{m}) \qquad (13)$$

with the location of the pole 0 of the logarithmic spiral at $X_c=1.0$ m and $Y_c=9.8$ m, and the friction angle $\phi=40.5°$. The effect of shear forces perpendicular to the direction of the nails was ignored in the limit equilibrium

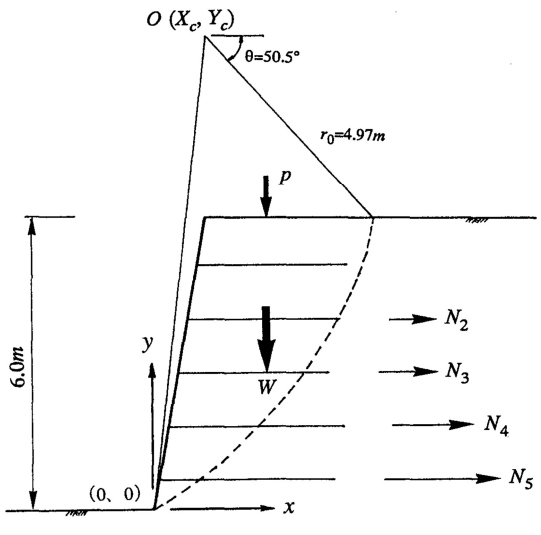

Fig. 17. Failure conditions in the prototype wall test

Table 3. Stability analysis for the prototype wall

Row i	L_i (m)	$(L_e)_i$ (m)	Lower bound T_{mi} (KN/m)	Lower bound N_i (KN)	Upper bound T_{mi} (kN/m)	Upper bound N_i (KN)
1	3.0	0	—	—	—	—
2	3.0	0.1	45	4.5	65	6.5
3	3.0	0.6	30	18	48	28.8
4	3.5	1.8	15	27	21.5	38.7
5	3.5	2.8	15	42	17.5	49
				Σ=91.5		Σ=123.0

analysis, as discussed by Pedley (1990). The friction angle between the shotcrete facing and soil was assumed to be $\delta_w = 3\phi/4 = 30°$. The location of the centroid of earth pressure was taken at $2/3H$ (hydrostatic distribution) from the observed earth pressures on the facing.

The total required force T_{req} per horizontal nail spacing (1.2 m) was calculated as 113.0 kN. The total measured horizontal earth-pressure force behind the shotcrete facing was P_h=80–90 kN/(1.2 m). Coulomb's theory, on the other hand, gives T_{req}=120.8 kN/(1.2 m), which is very close to the value calculated from the logarithmic spiral. Table 3 gives details of the estimates of the total available force T_{ava} based on the lower and upper bounds of the ultimate mean shear force $(T_m)_i$ from in-situ pull-out tests reported by Gassler (1987) for the corresponding depth of the nails. For the lower and upper bounds the values of T_{ava} are 91.5 and 123.0 kN respectively (per 1.2 m width), giving apparent factors of safety against T_{req} of 0.81 and 1.09. The average factor of safety $(F_s)_{ave}$ for these upper and lower bound is 0.95; this calculated factor of safety is very close to F_s=1.00 in the state of limit equilibrium, and shows that a good prediction could be made regarding the failure of the in-situ nailed slope. This supports the applicability of the limit equilibrium analysis for soil nailing, when accurate values for the friction angle of the soil and the maximum pull-out forces of nails are used in the analysis.

CONCLUSIONS

A series of centrifuge tests have been carried out on model soil-nailed walls with vertical and near-vertical faces. The failure surfaces were seen to have the shape of logarithmic spirals, and limit equilibrium analyses based on such surfaces were found to agree well with the observed failures. Failure in all cases was due to pull out of nails, rather than their breakage; significant bending of the nails only occurred after failure of the slope, and the analyses assumed only tensile forces in the nail, with shear and bending effects negligible. Prior to failure, measured earth pressures on the back of the wall facing compared reasonably well with those calculated by Coulomb's method. However the pressures at the base of the wall were less than calculated, and the line of action of the resultant force consequently somewhat higher.

Peak pull-out resistance and load-displacement data for the nails were obtained from a parallel series of small-scale pull-out tests. These allowed calculations to be made of wall displacements as well as failure conditions, and again the agreement with the centrifuge tests was reasonable. From the wall displacements, use of a simple velocity (displacement) field in the soil allowed calculations to be made of the ground movements behind the facing; these agreed reasonably well with the measured surface settlements.

Although the scale of the models was small, and the excavation process could not be properly modelled in the centrifuge tests, comparisons with a full-scale prototype test were sufficiently good to give confidence in the applicability of the model test results.

ACKNOWLEDGEMENTS

The first Author was given leave of absence and supported financially by his employers, Tokyu Construction Co. of Japan, during his time as a research student in Oxford; the company also provide funding for the experimental work, and their support is gratefully acknowledged. Thanks are due to Harvey Skinner of the Geotechnical Engineering Research Centre, City University, for his care and assistance with the centrifuge test programme. Thanks are also due to Professor Fumio Tatsuoka at the University of Tokyo and Professor Toru Kanda at the Tokyo Metropolitan University for their helpful advice.

REFERENCES

1) Bolton, M. D. (1986): "The strength and dilatancy of sands," Géotechnique, Vol. 36, No. 1, pp. 219–226.
2) Bolton, M. D. (1990): "Reinforced soil: Laboratory testing and modelling," Proc. of the Int. Reinforced Soil Conf., Glasgow, pp. 287–298.
3) Bolton, M. D., Choudhury, S. P. and Pang, P. R. L. (1978): "Reinforced earth walls: a centrifugal model study," Proc. of Symp. on Earth Reinforcement, Pittsburg, pp. 252–281.
4) Bolton, M. D. and Pang, P. R. L. (1982): "Collapse limit states of reinforced earth retaining walls," Géotechnique, Vol. 32, No. 4, pp. 349–367.
5) Bransby, P. L. and Milligan, G. W. E. (1975): "Soil deformation near cantilever sheet pile walls," Géotechnique, Vol. 25, No. 2, pp. 175–195.
6) Garg, K. G. (1992): "Evaluating soil-reinforcement friction," Proc. of Int. Symp. on Earth Reinforcement Practice, Vol. 1, Fukuoka, pp. 67–72.
7) Gassler, G. (1987): "Vernagelte Gelandesprunge-Tragverhalten und Standsichrheit," Ph.D. thesis, Univ. of Karlsruhe.
8) Gassler, G. and Gudehus, G. (1983): "Soil nailing-statistical design," Proc. of 8th Euro. Conf. on SMFE, Vol. 2, Helsinki, pp. 491–494.
9) Ho, S. K. and Rowe, R. K. (1992): "Finite element analysis of geosynthetic reinforced soil walls," To appear in Geosynthetic Conference, '93 Vancouver.
10) Jaber, M. B. (1989): "Behaviour of reinforced soil walls in centrifuge model tests," Ph.D. thesis, Univ. of California at Berkeley.
11) Jaky, J. (1944): "The coefficient of earth pressure at rest," J. of the Society of Hungarian Architects and Engineers, pp. 355–358.
12) Jones, C. P. D. (1990): "In-situ techniques for reinforced soil,"

Proc. of the Int. Reinforced Soil Conference, Glasgow, pp. 277–282.
13) Leschinsky, D. (1992): "Issues in geosynthetic-reinforced soil," Special & Keynote Lectures, International Symposium on Earth Reinforcement Practice, Fukuoka, Vol. 1, pp. 117–143.
14) Milligan, G. W. E. (1974): "The behaviour of rigid and flexible retaining walls in sand," Ph.D. thesis, Univ. of Cambridge.
15) Ovesen, N. K. (1984): "Centrifuge tests of embankments reinforced with geotextiles on soft clay," Proc. of Int. Symp. on Geotechnical Centrifuge Model Testing, pp. 14–21.
16) Pedley, M. J. (1990): "The performance of soil reinforcement in bending and shear," DPhil. thesis, Univ. of Oxford.
17) Plumelle, C., Schlosser, F., Delage, P. and Knochenmus, G. (1989): "French national research project on soil nailing. Design and performance of earth retaining structures," ASCE Geotechnical Special Publication, pp. 660–675.
18) Santamarina, J. C. (1984): "Effect of adjacent soils on reinforced soil structures-centrifuge model testing," MSc. thesis, Univ. of Maryland.
19) Shen, C. K., Kim, Y. S., Bang, S. and Mitchell, J. F. (1982): "Centrifuge modelling of lateral earth support," J. of the Geotech. Engrg. Div., Vol. 108, No. 9, pp. 1150–1164.
20) Stewart, D. I. (1990): "Groundwater effects on in-situ walls in stiff clay," Ph.D. thesis, Univ. of Cambridge.
21) Taniguchi, E., Koga, Y. and Yasuda, S. (1987): "Centrifugal model tests on geotextile reinforced embankments," Proc. 8th Asian Regional Conf. on SMFE, pp. 499–502.
22) Tatsuoka, F. (1987): "Discussion on strength and dilatancy of sand," Géotechnique, Vol. 37, No. 2, pp. 219–225.
23) Tei, K. (1993): "A study of soil nailing in sand," DPhil. thesis, Univ. of Oxford.
24) Terzaghi, K. and Peck, R. B. (1948): Soil Mechanics in Engineering Practice, John Wiley & Sons, New York.
25) Tufenkjian, M. R. and Vucetic, M. (1992): "Seismic stability of soil nailed excavations," Proc. of Int. Symp. on Earth Reinforcement Practice, Fukuoka, Vol. 1, pp. 573–578.
26) Yoo, N. J. (1988): "Centrifugal model experiments of reinforced earth retaining walls," Ph.D. thesis, Univ. of Colorado, Boulder.